AIAA Guidance, Navigation and Control Conference and Exhibit
20 - 23 August 2007, Hilton Head, South Carolina

AIAA 2007-6447

Central East Pacific Flight Scheduling

Shon Grabbe* and Banavar Sridhar†
NASA Ames Research Center, Moffett Field, CA, 94035-1000

Avijit Mukherjee ‡
University of California Santa Cruz, Moffett Field, CA, 94035-1000

This paper examines the implications of strategically scheduling flights on user-preferred routes in the Central East Pacific to reduce trajectory crossing points. After first casting the flight scheduling problem in terms of a job shop scheduling problem, a 0-1 integer programming model is used to calculate the optimal departure and en route controls required to generate feasible flight schedules. To enhance the solution, a ration-by-schedule based heuristic is introduced to transform the original model into a subset of problems. By varying attributes of the machines in the job shop scheduling formation, two distinct types of feasible schedules are obtained. The first type of schedules are highly restrictive yet but free of all four-dimensional trajectory crossing points, while the second type are less restrictive but may require limited tactical flight separation maneuvers to alleviate residual crossing points. The average adjusted time savings per flight varied between 1.8 minutes and 4.6 minutes per flight when allowing for both strategic flight scheduling and user-preferred flight routing.

I. Introduction

The overarching viewpoint that is influencing how future air traffic services are provided under the Joint Planning and Development Organization's (JPDO's) Next Generation Air Transportation System (NGATS) is to "accommodate user preferences to the maximum extent possible."[1] Work contributing to this vision in the oceanic domain is underway at several research organizations.[2,3,4] For example, recent efforts have focused on providing enhanced situational awareness to pilots to enable more frequent step-climbs and to increase awareness of surrounding traffic.[3] Additionally, in Ref. 4 a backward recursion dynamic programming algorithm was utilized to calculate minimum-time wind-optimal routes, which served as surrogates for the actual user-preferred routes, in the Central East Pacific (CEP). This study showed that significant benefits could be achieved by transiting flights off the fixed CEP-based route structure onto wind optimal routes particularly during the winter months when the polar jet stream commonly intersects the CEP routes.

The one major concern raised in this study related to the significant number of new simulated, four-dimensional (4-D) trajectory crossing points that were generated as a result of allowing user-preferred routing in this region of the ocean. In this study, a 4-D trajectory crossing point is defined as a point in which two or more flights are predicted to co-exist at the same location in space (latitude, longitude, and altitude) and time. An example of several potential 4-D trajectory crossing points is highlighted by the squares in Fig. 1b. These additional crossing points may significantly increase the workload of the air traffic controllers that would be managing these new traffic streams, since these crossing points would require close monitoring to avoid the potential for loss-of-separation. For reference, the simulated flight histories for all eastbound flights that utilized one of the seven CEP routes on Dec. 14, 2005 are shown in Fig. 1a. By contrast, the same set of flights on simulated wind optimal routes are shown in Fig. 1b. The wind-optimal routes depicted in this figure were generated using the technique described in Ref. 4 in which flights traveled along their nominal routes in domestic airspace, and wind optimal routes only within oceanic

* Research Scientist, Automation Concepts Research Branch, Mail Stop 210-10, Shon.R.Grabbe@nasa.gov, AIAA Member.
† Chief, Automation Concepts Research Branch, Mail Stop 210-10, Fellow AIAA.
‡ Associate Project Scientist, University of California, Santa Cruz, Mail Stop 210-8.

airspace. Had the complete wind optimal routes between the origin and destination been depicted, considerably more 4-D trajectory crossing points would occur. The most noticeable difference between the flight histories depicted in these two images results from the fact that the highly structured CEP routes ensures that flights on parallel tracks remain laterally separated, which is not the case when flights are allowed to fly along wind-optimal routes.

The purpose of this paper is to describe a general approach for scheduling flights in the aforementioned 4-D trajectory crossing point problem. This study is believed to be the first to examine the potential benefits of allowing flights to travel on user-preferred-routes in the CEP, while strategically scheduling these flights to ensure that the number of trajectory crossing points is manageable. The issue of whether user-preferred trajectories are beneficial in the CEP is an open research area that is outside the scope of the current study.

At the core of this new technique, is a novel approach for transforming the flight scheduling problem into a job shop scheduling problem.[5] Literature on the job shop dates back to the fifties and sixties[7] and has received widespread use in the manufacturing and service industries,[8] and more recently in the semiconductor industry[9] for scheduling and planning operations. The basic premise behind the job shop scheduling approach is the need to schedule a set of jobs, which could be flights or patients in a hospital, to a set of machines, which could be regions of airspace or hospital beds. A more detailed discussion of the job shop scheduling formulation used in this study is reserved for Section II.A. The resulting job shop scheduling problem is subsequently solved using a 0-1 integer programming model that was originally developed to solve a deterministic traffic flow management problem.[6] By varying the attributes of the machines in the job shop scheduling problem, two distinct types of feasible schedules are generated. The first type of schedules are highly restrictive but ensure that all 4-D trajectory crossing points are eliminated, while the second type are less restrictive yet may require a limited amount of tactical flight separation to eliminate all crossing points. The issue of how the tactical flight separation would be accomplished in a futuristic air traffic control (ATC) system is an open research area that would likely require changes in ATC procedures and the development of new advanced ground-based and flight-deck based technologies, such as those described in the Distributed Air/Ground (DAG) Traffic Management (TM) operational concept.[10]

To test this new scheduling approach, the flights that were nominally scheduled to fly along one of the seven structured CEP based routes on Dec. 14-16 and 19-20 of 2005 (see Fig. 1a) were first rerouted using the minimum travel time, wind-optimal routing algorithm described in Ref. 4, and then scheduled using the approach described in this study. The resulting flight schedules are examined in terms of the scheduling delays, the number of residual trajectory crossing points, and the adjusted time savings.

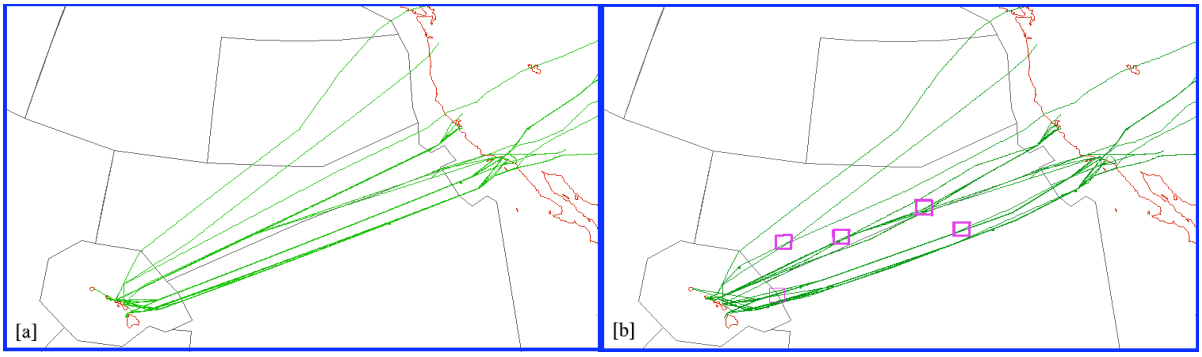

Figure 1. Flight histories for [a] eastbound nominal Central East Pacific (CEP) routes and [b] eastbound oceanic wind-optimal CEP routes on Dec. 14, 2006.

Section II provides a high level overview of the job shop scheduling problem within the context of flight scheduling. The 0-1 integer programming model that was adopted for this study, as well as a heuristic for decomposing this model into a number of computationally tractable sub-problems is also discussed in this section. Statistics related to the job shop formulation of the flight scheduling problem as well as the flight scheduling results are presented in Section III. Section IV contains concluding remarks and recommendations for future research.

II. Modeling Method

To strategically resolve the temporal trajectory crossing points, this study begins by recasting the CEP routing problem, which consists of flights, sectors, and schedule travel times, in terms of the job shop scheduling problem that consists of jobs, operations, schedules, and machines. This mapping enables the utilization of integer programming and graph-based solution methodologies for calculating airborne and departure delays that resolve the 4-D trajectory crossing points. The remainder of this section is formatted as follows. In Section II.A, the job shop scheduling formulation of the CEP routing problem is presented; the 0-1 integer programming model adopted is presented in Section II.B; and finally a heuristic for decomposing this model into computationally tractable sub-problems is presented in Section II.C.

A. Job-Shop Formulation

The job shop problem consists of a set of N jobs $\{J_i | i = 1,...,N\}$ and a set of m machines $\{M_k | k = 1,...,m\}$. Each job can only be processed on one machine at any given instance of time, and each machine can only process one job at a given instance of time. Jobs are further subdivided into a sequence of P_i operations that are subsequently processed at one of the available machines.[5] As an example, the set of operations associated with the i^{th} job can be denoted as $\{O_{ij} | i = 1,...,N \text{ and } j = 1,...,P_i\}$. Here the first subscript denotes the job number and the second subscript denotes the operation index. This set of operations also contains precedence constraints, which require that operation O_{ij} be completed prior starting work on operation O_{ij+1} for all $j = 1,...,N_i$. Furthermore, each operation requires processing time l_{ij} on a particular machine $M_{ij} \in \{M_1,...,M_m\}$. The objective of the job shop problem is therefore to find a feasible solution (i.e., one for which each operation O_{ij} is scheduled to a machine M_{ij} subject to the aforementioned constraints) that minimizes a particular cost function.

In terms of the oceanic flight scheduling problem, each flight can be thought of as a job, and each machine represents a region of oceanic airspace. To facilitate this study, a uniform three-dimensional grid was overlaid on Oakland Oceanic Sectors 3 (OC3) and 4 (OC4), which are the primary oceanic sectors through which flights on the CEP routes travel (see Fig. 2). For this initial study, no attempt was made to define an "optimal" grid that accounted for the prevailing easterly and westerly traffic flows in this region. Follow-on studies that examine the benefits of creating sparse grids that are aligned with the traffic flows would be beneficial. It is worth noting that this process of overlaying a grid on a region of airspace has been used in the past,[11,12] but the current application to oceanic flight scheduling is believed to be unique. A graphical representation of the resulting airspace is shown in Fig. 2. Depicted in this figure are the Hawaiian Islands in the lower left corner, the west coast of the United States on the right side, the OC3 and OC4 boundaries, a representative grid with corresponding cell (i.e., machine) labels, and two wind optimal routes.

In this study, two different horizontal grid cell sizes were used to explore the scalability and dimensionality of the flight scheduling approach. The first grid cell size was 30 nautical miles (nmi) by 30 nmi, which corresponds to the soon to be operationally implemented lateral and longitudinal separation standard for flights on the CEP routes. The number of operations that were allowed to be scheduled to each of the machines corresponding to one of these cells was assumed to be one, which ensured that no two flights occupied the same machine, or 30 nmi x 30 nmi region of airspace at any time. The second grid cell size was 100 nmi by 100 nmi, which has two primary benefits. Firstly, the larger grid cell size reduces the effective number of machines that each flight must utilize, which significantly reduces the computational complexity of the scheduling problem as will be shown in Section 3. Secondly, the capacity of each of these larger machines (i.e., regions of airspace) was also assumed to be greater than 1, which allowed more than one flight to occupy the machine at any instant. The main reason for allowing this is because these schedules will be less restrictive than the schedules generated with the smaller grid cells that only accommodate a single flight at any instance of time. The vertical dimension of each cell was set to 1,000 ft, which corresponds to the vertical separation of flights along the CEP routes.

Continuing with the job shop analogy, each grid cell depicted in Fig. 2 will become a machine in the problem formulation, and each flight path will be decomposed into a series of operations by transforming the continuous flight plan into a set of discreet events. As an example, job 1, J_1, which is composed of operations $\{O_{1q} | 1 \le q \le 10\}$ utilizes the following subset of machines: $\{M_{48}, M_{47}, M_{38}, M_{37}, M_{36}, M_{28}, M_{27}, M_{19}, M_{18}, M_9\}$, where O_{11} is processed on M_{48}, O_{12} is processed on M_{47}, etc. For clarity, the first two operations associated with job one, J_1, which are labeled O_{11} and O_{12}, are explicitly in Fig. 2. Similarly, job two, J_2, which is represented by the lowermost

flight path in this figure is composed of operations $\{O_{2q} | 1 \le q \le 8\}$ and these eight operations are processed on the following subset of machines:
$\{M_{32}, M_{31}, M_{30}, M_{29}, M_{20}, M_{19}, M_{18}, M_9\}$. The processing time, l_{ij}, associated with operation O_{ij} will therefore be the time required for a given flight to traverse grid cell C_{ij}.

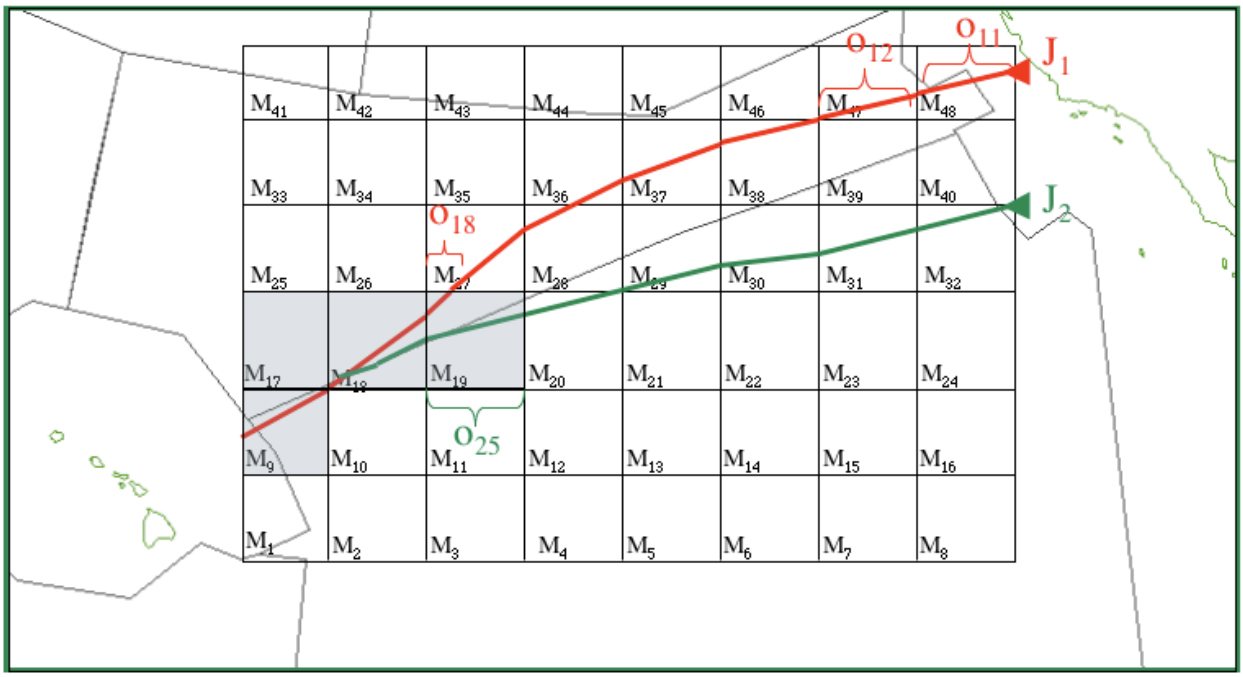

Figure 2. Central East Pacific with representative oceanic grid.

After casting the flight scheduling problem in terms of the job shop problem, the objective is to find a feasible solution that temporally spaces flights to eliminate 4-D trajectory crossing points subject to a specified cost function. The light, bluish-grey cells in Fig. 2 illustrate three potential trajectory crossing points. Assuming that both jobs J_1 and J_2 require access to machine M_{19} at time t', a Gantt chart can be used to depict a subset of both a nominal schedule (see Fig. 3a) and a potentially feasible schedule (see Fig. 3b). If the processing time of the eight operations associated with J_1 (i.e., O_{18}) is l_{18} and the processing time of the fifth operation associated with J_2 (i.e., O_{25}) is l_{25}, then a potentially feasible schedule can be obtained by increasing the processing time of O_{25} to $l'_{25} = l_{25} + l_{18}$. From a flight scheduling perspective, this would require the flight corresponding to J_2 to absorb $\Delta t = l_{18}$ units of time prior to reaching machine M_{19}. This could be done through a combination of pre-departure delays, speed controls, or path stretching. Sections II.B describe the algorithmic approaches that were adopted in this study for calculating feasible flight schedules.

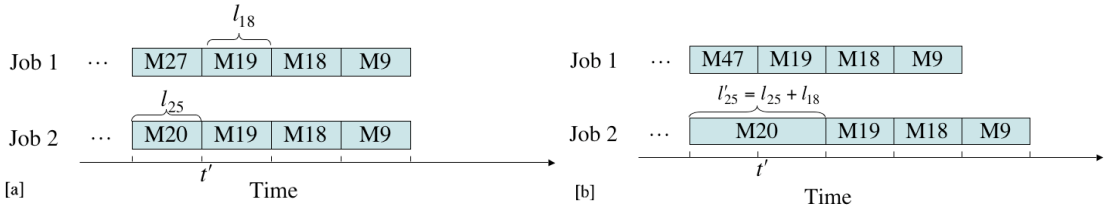

Figure 3. Illustrative [a] unscheduled and [b] scheduled Gantt charts for four jobs and five machines.

B. 0-1 Integer Programming Model

To schedule the CEP flights, the 0-1 integer programming model that was originally described in Ref. 6 was adopted, and is summarized here for completeness. It is worth noting that this is a general model that has been

developed for assigning optimal delays to flights in order to satisfy airspace capacity constraints, such as airport arrival rate or sector capacity constraints. This model relies upon a binary decision variable $w_{ft}^{j} \in \{0,1\}$ that is defined as follows:

$$w_{ft}^{j} = \begin{cases} 1, \text{ if flight f arrives at sector j by time t} \\ 0, \text{ otherwise} \end{cases}$$

With this definition of w_{ft}^{j}, the objective of this model is to minimize the total delay cost with respect to the unconstrained schedule that is expressed as follows:

$$\min \sum_{f \in F} \left[(c_f^g - c_f^a) \sum_{\{t \in T_f^k \mid k = P(f,1)\}} t(w_{ft}^k - w_{f,t-1}^k) + c_f^a \sum_{\{t \in T_f^k \mid k = P(f,N_f)\}} t(w_{ft}^k - w_{f,t-1}^k) \right] \quad (1)$$

The first summation in this expression is over all flights (i.e., jobs in the job shop scheduling parlance), the second summation is over all times that a given flight could occupy the departure airport, while the third summation is over all times that a flight can land at the destination airport. The expression $(w_{ft}^{j} - w_{f,t-1}^{j})$ is defined to be one if flight f arrives at sector j at time t, and is zero otherwise. As is commonly done, airborne delay costs, c_f^a, were assumed to be twice as large as departure delay costs, c_f^g. N_f is the number of sectors in the path of flight f; $P(f,i)$ represents the flight path of flight f where $P(f,1)$ is the origin and $P(f,N_f)$ is the destination; F is the set of all flight; and T_f^k is the set of feasible times that flight f can occupy airport k. This expression is minimized with respect to the following set of constraints:

Sector Capacity: Ensures that demand in sector j at time t does not exceed the sector's time-varying capacity,

$$\sum_{\{(f,j') \mid P(f,i) = j, P(f,i+1) = j', i < N_f\}} (w_{ft}^{j} - w_{ft}^{j'}) \le S_j(t), \ \forall j \in J, \ t \in T \quad (2)$$

Within the job shop scheduling context, each machine corresponds to a sector within this model; J corresponds to the set of all machines; and T is the set of all time periods considered in the scheduling problem. For our study, machine capacities, $S_j(t)$, were varied between one and three. A machine capacity of one ensured that only one operation (i.e., flight) could occupy any given machine at a instance of time, which prevented 4-D trajectory crossing points from occurring. Machine capacities of two and three were also permitted in this study for the machines represented by the 100 nmi x 100 nmi region of airspace. These increased machine capacities result in fewer binding constraints in the optimization problem, but can also lead to situations in which multiple flights utilize a common machine at the same time, which can lead to a limited number of unresolved 4-D trajectory crossing points.

Sector Connectivity: Ensures that flight f must spend at least l_{fj} units of time in sector j before proceeding to sector j' if j and j' are consecutive sectors along the path of flight f,

$$w_{f,t+l_{fj}}^{j'} - w_{ft}^{j} \le 0, \forall f \in F, \ t \in T_f^j, \ j = P(f,i), \text{ such that } i < N_f, \text{ and } j' = P(f,i+1) \quad (3)$$

Time Connectivity: Requires that if a flight has arrived at sector j by time t, then w_{ft}^{j} has a value of 1 for all later time periods,

$$w_{ft}^{j} - w_{f,t-1}^{j} \ge 0, \ \forall f \in F, \ j \in P_f, \ t \in T_f^j \quad (4)$$

It is worth noting that the original model presented in Ref. 6 also includes a set of arrival capacity, departure capacity, and flight connectivity constraints that are used to handle flight connectivity. Since these constraints were not relevant to the current en route flight scheduling problem, their description has been omitted. To illustrate the

use of this model, the wind-optimal routes for east- and westbound CEP flights will be scheduled to minimize 4-D trajectory crossing points.

C. Scheduling Heuristic

According to Ref. 6, an upper bound on the number of variables w_{ft}^{j} and the number of constraints for the model described in Section II.B is given by the following equations $\mathrm{F}\cdot\mathrm{D}\cdot\mathrm{X}$ and $2\cdot K\cdot T + J\cdot T + 2\cdot F\cdot D\cdot X + C\cdot D$, respectively. Here F is the total number of flights, T is the total number of time periods (in minutes for this study), J is the total number of sectors, K is the total number of airports, C is the total number of continued flights, D is the maximum cardinality, or number of elements, of the set of feasible times for flight *f* to be in sector *j*, and X is the maximum number of sectors (i.e., machines) that a flights passes through. The values of each of these parameters and the upper bounds on the number of variables and constraints for a typical problem encountered in this study is shown in the row labeled "Full Problem" in Table 1. As can be seen from this table, the upper bound on the number of variables and especially the number of constraints can grow exceedingly large. This is due in part to the long time horizon, T=1,800 minutes, and the number of machines involved, J = 9,000, associated with scheduling a days worth of CEP flights. To put the number of machines (i.e., regions of airspace) involved in this study in perspective, there are roughly 800 sectors covering the airspace associated with the 20 Centers that cover the contiguous United States. The row labeled "Sub problem" will be described in detail later in this section.

	D	X	F	T	K	J	C	Variable Upper Bound	Constraint Upper Bound
Full Problem	100	100	170	1,800	40	9,000	0	1,700,000	19,744,000
Sub problem	100	100	30	600	40	1,100	0	300,000	1,308,000

Table 1. Upper bound on the number of variables and constraints for a typical 30 nmi grid scheduling problem.

The most effective way to reduce the computational complexity associated with the size of the scheduling problem that was encountered in this study was to (1) reduce the number of machines, J; or (2) reduce the number of time periods, T. Reducing the number of machines, J, involves either increasing the area of coverage of each machine, which is the approach taken in this paper, or developing a sparse collection of specialized machines that accounts for the prevailing traffic flows. Although the former of these two approaches was taken for the current study, future research that addresses the latter of these two approaches would be beneficial. Reducing the number of time periods, T, can be accomplished by either increasing the time step, or partitioning the problem into a number of sub-problems while maintaining the one-minute step size used in this study. Increasing the time step beyond one minute would have greatly decreased the resolution of the grid-based trajectories, which was undesirable for the current application. Therefore the following heuristic was developed to divide the original scheduling problem into a set of N computationally tractable problems to alleviate the temporal factors influencing the computational complexity.

Step 1: Flight Partitioning

Partition the original set of *N* flights into a set of N_{sub} flights $\{\mathrm{F_i}|\mathrm{i}=1,...,\mathrm{N_{sub}}\}$. For this study, the set of flights was subdivided by leveraging the ration by schedule (RBS) concept that is an integral component of the Federal Aviation Administration's ground delay program (GDP).[13] For GDPs, rationing of arrival resources is based on the schedule arrival times of flights, whereas in this study the rationing is based on the scheduled oceanic entry time for each flight. For this study, the flights are assumed to fly on their nominally scheduled routes in the domestic airspace and wind optimal routes in the oceanic airspace. Therefore, the aforementioned oceanic entry point corresponds to the position at which the structured domestic route intersects the horizontal grid that has been overlaid on the CEP. More details regarding this horizontal grid are presented in Section III.A. As a result of the rationing employed in this heuristic, the first *n* flights that are scheduled to enter the oceanic airspace will appear in $\mathrm{F_1}$, the next *n* flights will appear in $\mathrm{F_2}$. This procedure is continued until the original set of *N* flights has been

allocated to one of the N_{sub} subset of flights. Corresponding to each subset of flights, a subset of machines $\{J_i \mid i = 1,...N_{sub}\}$, and time intervals $\{T_i \mid i = 1,...N_{sub}\}$ is generated.

Step2: Flight Scheduling
Solve Eqs. (1)-(4) using the i^{th} subset of flights F_i, machines J_i, and times T_i, and store the resulting machine demand $\overline{D}_k^i(t)$ that can be obtained from Eq. (2).

Step 3: Adjust Cell Capacity
If additional flights remain to be scheduled after the i^{th} stage, then reduce the cell capacity, $S_j(t)$, appearing in Eq. (2) for the $(i+1)^{th}$ set of flights that remain to be scheduled and repeat Step 2, otherwise terminate. The resulting residual cell capacity will be given by $S_j(t) = \max\left(S_j(t) - \sum_{l=0}^{i} \overline{D}_k^l(t),\ 0 \right)$.

Using the heuristic outlined above, the original CEP scheduling problem was reduced to a series of six smaller sub-problems. The upper bound on the number of variables and constraints that were encountered in the sub-problems when a 30 nmi grid was used are shown in Table 1. It is important to note that because of the problem formulation, the upper bound on the number of variables increases from $F \cdot D \cdot X$ to $F \cdot D \cdot X + (N-1) \cdot J \cdot T$. This increase is due to the fact that the sector demand variables, which are mentioned in Step 2, have been cast as variables here. Future efforts should address modifications to the current scheduling heuristic that reduce the upper bound on the number of variables. The "Sub problem" results in Table 1 therefore reflect variable counts for the first stage of the sub-divided problem. As can be seen from this table, this approach is an effective means by which the upper bound on the number of variables and constraints can be reduced by a factor of 50 and 25, respectively. Results utilizing this heuristic are shown in Section III.B. An in-depth investigation into the optimality gap between the true optimal solution and the solution resulting from this heuristic is outside the scope of the current study, but will be investigated in a follow on research effort.

III. Results

The set of flights was extracted from historical Aircraft Situation Display to Industry (ASDI)[14] data for Dec. 14-16 and 19-20 of 2005. Using the wind fields from the Global Forecast System (GFS) Atmospheric Model[15] and the algorithm for generating "oceanic center boundary (OCB)" wind-optimal routes that is defined in Ref. 4, routes were calculated for each of the flights, whose scheduled flight plan nominally utilized one or more of the seven CEP routes depicted in Fig. 1a. For reference, the wind-optimal routes calculated in Ref. 4 make use of a backward recursion, minimum-travel-time dynamic programming algorithm. An example of the simulated wind-optimal flight tracks from Dec. 20, 2005 between the Hawaiian Islands and the west coast of the United States mainland is shown in Fig. 4a.

Before the model that is described in Section II.B can be used to schedule the flights, the 4-D flight trajectories must first be converted from the discrete time varying latitude, longitude, altitude, system (λ, τ, z, t) to the time varying, grid based system that involves a row index *i*, a column index *j*, and a flight level index *k*, (i, j, k, t). This method was discussed in Section II.A and examples of the trajectories on a 30 nmi grid and a 100 nmi grid are presented in Fig. 4b and 4c for all CEP flights that were scheduled to fly on Dec. 20, 2005. Note that two-dimensional projections are being used for display purposes, whereas the actual scheduling calculations utilized the three-dimensional grid based trajectories as input, and produced the 4-D flight trajectories (time being the 4^{th} dimension) as output. Recall that the 30 nmi grid is being used here, because this will soon be the lateral and longitudinal separation standard in the CEP. The 100 nmi grid is being used because it substantially reduces the number of cells/machines that each flight is required to pass through, which in turn reduces the dimensionality of the integer programming-based scheduling model that is being solved. Additionally, the 100 nmi grid is large enough to potentially accommodate two to three flights at any given instance of time. After the job scheduling process, any trajectory crossing points within these larger grid cells could be resolved using tactical ground-based, or flight deck based tactical separation maneuver strategies.

The remainder of this section is structured as follows. In Section III.A, characteristics regarding the number of machines, jobs, and operations, associated with the unscheduled flight trajectories will be discussed, so the reader

gains an appreciation for the magnitude of the problem being considered in this study. Results from the scheduling algorithm that make use of the heuristic described in Section II.C are presented in Section III.B.

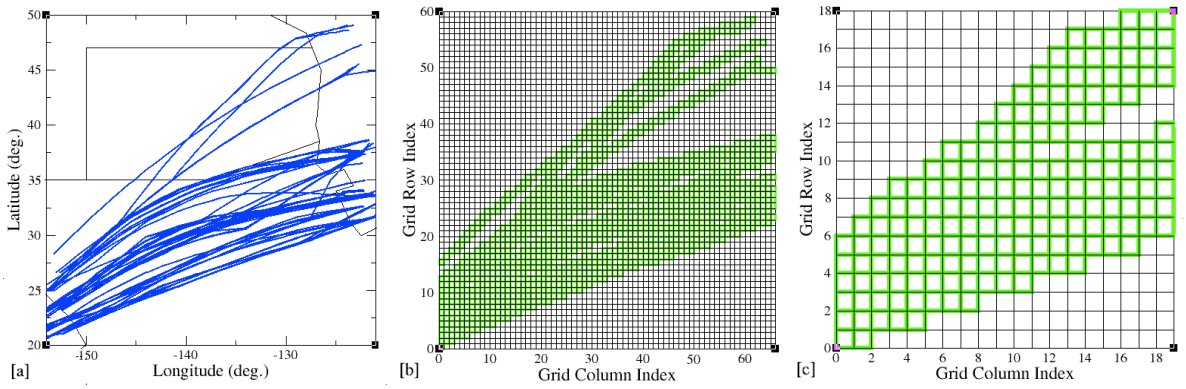

Figure 4. [a] Oceanic wind optimal flight tracks, [b] tracks on 30 nmi grid, and [c] tracks on 100 nmi grid for Dec. 20, 2005.

A. Unscheduled Machine, Job, Operation, and Usage Statistics

The unscheduled machine, job, operation, and occupancy statistics for Dec. 14-16 and 19-20, 2005 are presented in Tables 2 and 3 for both the 30 nmi grid and 100 nmi grid, respectively. Here "unscheduled" indicates that all flights are on wind-optimal routes, and no attempt has been made to eliminate or reduce the number of 4-D trajectory crossing points using the scheduling approach described in Section II. Recall that within the current job-shop scheduling formulation, a machine refers to a region of airspace (either 30 nmi x 30 nmi or 100 nmi x 100 nmi); a job refers to a flight; and a flight plan is decomposed into a series of operations each of which is processed by a single machine. The horizontal grid used in this study ranged from 20^{O} to 50^{O} north latitude and from 121^{O} to 154^{O} west longitude, while the vertical grid extended from flight level 180 to flight level 400 in increments of 1,000 feet. For reference, the horizontal grid used in this study was roughly 1,500 nmi wide by 1,800 miles long. By comparison, a rectangular grid placed over the contiguous U.S. is roughly 2,600 nmi wide by 1,400 nmi long. Therefore the area over which flights were being scheduled covered a region of airspace that was roughly three-quarters of the size of the contiguous U.S. The theoretical upper bounds on the number of machines (i.e., cells) that could be used for the 30 nmi and 100 nmi cases were 87,120 and 7,254, respectively. As can be seen by comparing these figures with the actual machine counts that appear in Tables 2 and 3, only about 3% of the available machines were used with the 30 nmi grid and roughly 6% of the machines were used with the 100 nmi grid case.

Date	Machine Count (Airspace Regions)	Job Count (Flights)	Machines with Occupancy ≥ 2	Instances Machine Occupancy ≥ 2	Average Operations per Job
12/14/05	2,457	150	329	1,089	78
12/15/05	2,528	157	224	479	79
12/16/05	2,628	206	300	1,027	81
12/19/05	2,559	195	256	719	81
12/20/05	2,210	175	316	704	81

Table 2. Unscheduled machine, job, operation, and occupancy statistics for the 30 nmi grid.

The number of unique machines, and the total number of instances each of these machines exceed the capacities for both the 30 nmi and 100 nmi grids, are presented in the forth and fifth columns of Tables 2 and 3, respectively. For the 30 nmi grid, the maximum number of operations that can occupy any machine at an instance of time is one for this study, while for the 100 nmi grid the number of operations permitted in a machine was varied between two and three. As can be seen from the results in these tables, the total number of machines requiring scheduling

dramatically drops when the grid size is allowed to increase and the associated capacity of each machine is also allowed to increase. For the 30 nmi grid (see Table 2), roughly 10% of all machines required scheduling when the machine capacity was set to one. When the grid size was increased to 100 nmi and the capacity of each machine was two, the number of machines requiring scheduling varied between 8% and 15%, but when the machine capacity was increased to three the number of machines requiring scheduling only ranged between 2% and 5% of all machines. Note that a machine capacity of two or three indicates that two or three flights are allowed to use a machine (i.e., occupy the same region of airspace) at a given instance of time. Finally, the average number of operations per job decreased by roughly a factor of three when transitioning to the large grid. The decrease in machine count and operations per job associated with the 100 nmi grid is expected to significantly decrease the computational complexity of the integer programming scheduling model that is to be solved for these cases.

Date	Machine Count (Airspace Regions)	Job Count (Flights)	Machines with Occupancy		Instances Machine Occupancy		Average Operations per Job
			= 3	≥ 4	= 3	≥ 4	
12/14/05	494	150	61	22	742	96	25
12/15/05	451	157	36	10	272	26	26
12/16/05	437	206	63	8	607	29	26
12/19/05	445	195	47	22	553	56	27
12/20/05	383	175	57	7	397	35	26

Table 3. Unscheduled machine, job, operation, and occupancy statistics for the 100 nmi grid.

In addition to the aggregate machine occupancy statistics appearing in Tables 2 and 3, the total number of unscheduled operations that require use of a machine is also of interest and is displayed in Fig. 5. This information is beneficial for understanding average and maximum machine usage requirements. In addition, this information indirectly influences the computational complexity of the scheduling algorithm because of the presence of the sector capacity constraint that is defined in Eq. (4). When drawing this comparison, it is important to recall that the sector capacity in Eq. (4) is specified for a specific sector j and time t, whereas the results presented in Fig. 5 are machine occupancy statistics over an entire day. The most notable difference between the results presented in the two images in Fig. 5 is the maximum number of operations occupying each machine for the 30 nmi and 100 nmi grids. For the 30 nmi grid, each machine tends to process three or fewer operations per day, whereas in the 100 nmi grid case each machine tends to process 16 or more operations per day. Intuitively, these results are expected, because as the airspace is partitioned into large regions the number of operations that require processing in each region should also increase.

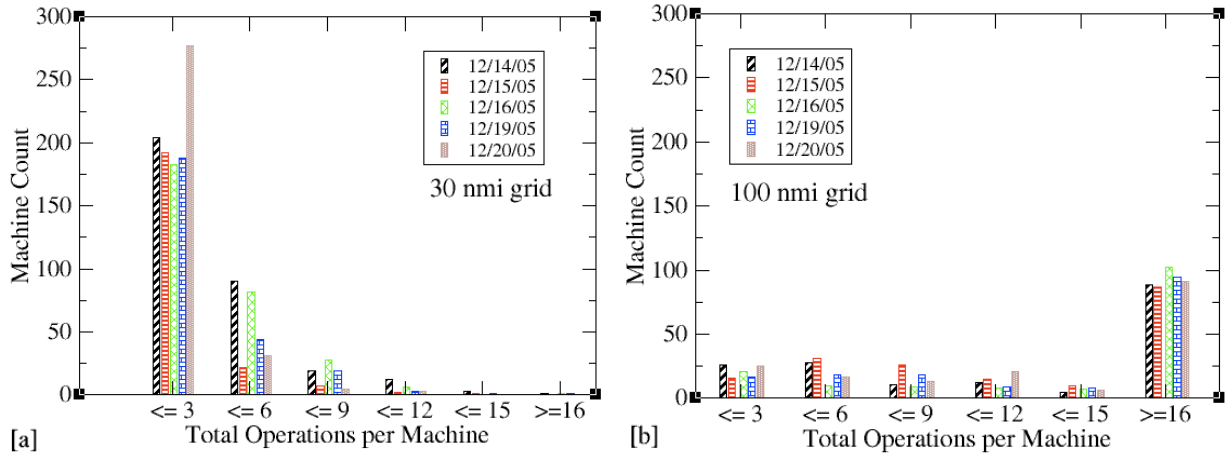

Figure 5. Total unscheduled operations per machine for [a] the 30 nmi grid and [b] the 100 nmi grid.

B. Scheduling Results

In this section, the results of scheduling the jobs (i.e., flights) that were discussed in Section III.A using the model and heuristic described in Sections II.B and II.C are presented using the Dec. 20, 2005 data set. Results from other days are expected to yield similar results. Three distinct sets of scheduling results were generated. For the first set of calculations, the 30 nmi grid was used with a cell capacity of one and the problem was divided into six sub-problems using the heuristic described in Section II.C. The second set of calculations utilized the 100 nmi grid with a machine capacity of two and this problem was also divided into six sub-problems. Finally, the third set of calculations utilized the 100 nmi grid with a cell capacity of three and again the problem was divided into six sub-problems. As previously discussed, the first set of calculations with the 30 nmi grid is believed to be the most restrictive yet will ensure that all trajectory crossing points are strategically eliminated through job scheduling. The second and third sets of calculations are believed to be less restrictive and allow for a limited number of trajectory crossing points to exist after scheduling, which would later be resolved through tactical separation maneuvers. None of these cases were solvable without first partitioning the original problem into a number of smaller sub-problems on the hardware that was available.

Before examining the scheduling results, it is informative to examine the implications of subdividing each of the aforementioned sets of scheduling calculations into sub-problems. In Table 4, the number of variables, constraints, and the runtime (as determined by the Unix "time" command) are presented for each of the 0-1 integer programming problems (see Section II.B) for the third set of calculations, for which the 100 nmi grid was used with a cell capacity of three. These calculations were performed on a Redhat Linux based-laptop computer with a 3.0 GHz Pentium 4 processor and 1 GB of RAM. All scheduling results were generated using AMPL/CPLEX (version 10.0) and the variable and constraint counts listed in Table 4 are values prior to AMPL's "presolve" phase. The total variable count for each stage reduces to less than 80,000 variables after the presolve phase, similarly the number of constraints never exceeds 280,000 after the presolve phase. For this problem, the upper bound on the number of variables and constraints for the full problem would have been 744,625 and 2,185,850, respectively. Similarly, after accounting for the additional sector demand variables in the sub-problem formulation, the upper bound on the number of variables and constraints for any one sub-problem would have been 4,191,625 and 2,185,850, respectively. This assumes K = 2, T = 1800, J = 383, D = 115, X = 37, and F = 175 for the expressions given in Section II.C. As can be seen from this table, subdividing the problem greatly reduced the size of each scheduling stage, and in fact none of the original scheduling problems could be run to their entirety on the hardware available for this study due to memory limitations.

Sub-problem	Integer Programming Variable Count	Integer Programming Constraint Count	Runtime (sec)
1	75,558	442,439	6.2
2	180,326	517,990	21.4
3	234,913	572,488	8.7
4	732,699	1,213,471	17.5
5	599,201	1,001,217	10.6
6	830,400	1,254,384	12.0

Table 4. 0-1 Integer programming variable, constraint, and timing information for the Dec. 20, 2005 data set with a 100 nmi grid, 6 sub-problems, and machine capacity of 3.

The total delays, machine occupancy, and adjusted total time savings for the 175 jobs (i.e., flights) that were scheduled on Dec. 20, 2005 are presented in Table 5. Here the adjusted time savings is equal to the time savings resulting from the wind-optimal routing minus the delay associated with scheduling the flights. By increasing the grid size from 30 nmi to 100 nmi and allowing simultaneous processing of multiple operations per machine, the total delays significantly decreased. For example, the delays decreased by nearly 70% when transitioning from the 30 nmi case with a capacity of one to the 100 nmi case with a capacity of two. This savings of course comes at the expense of leaving a significant number of 4-D trajectory crossing points unresolved in the 100 nmi case, which may require tactical flight spacing controls. A further order-of-magnitude reduction in the total delays was observed when the capacity of the 100 nmi grid cell was increased form two to three. It is also worth noting that all delays were absorbed on the ground for this scheduling case. As expected the number of machines requiring scheduling and the total number instances that machine intersections occurred which required scheduling dramatically reduced when moving from the 30 nmi grid to the 100 nmi grid. Finally, when an average "oceanic center boundary" wind-optimal time savings of 4.8 minutes is assumed for each job,[4] then the total adjusted time savings varied between 318 and 808 minutes, which corresponds to an average adjusted time savings of 1.8 and 4.6 minutes, respectively. Assuming an average airline operating cost of \$29/hr,[16] the combined routing and scheduling time savings translates

into an annual savings that ranges $3.4 million and $8.5 million. Any tactical resolutions required to alleviate 4-D trajectory crossing points in the 100 nmi grid case could further reduce the average per flight time savings. For this initial study, no attempt has been made to estimate the costs associated with these tactical maneuvers.

Scheduling Scenario	Total Delay (min)	Machines with Intersections		Instances of Machine Intersections		Adjusted Total Time Savings (min)
		Unscheduled	Scheduled	Unscheduled	Scheduled	
30 nmi, capacity=1	522	316	0	704	0	318
100 nmi, capacity=2	311	64	0	432	0	529
100 nmi, capacity=3	32	7	0	35	0	808

Table 5. Dec. 20, 2005 scheduling results for: (1) 30 nmi grid, six sub-problem, capacity=1; (2) 100 nmi, six sub-problems, capacity =2; and (3) 100 nmi grid, six sub-problems, capacity=3.

Although the average delay per job ranged from 3.0 minutes for the 30 nmi case to 0.18 minutes for the 100 nmi case with capacity equal to three, the actual per job delays were found to be far less equitable and unevenly distributed. These results are shown in Fig. 6 for the 175 jobs that required scheduling on this day for each of the three scheduling cases. As can be seen from this figure, the individual job delays were found to range from zero for a significant number of flights to 99 minutes for a single flight in one case. The largest job delay cases also tended to occur for jobs with the highest job index. This trend is to be expected since the flights with the larger job indices were some of the last to be scheduled, because of the heuristic that was employed in this study to subdivide the original scheduling problem into *N* smaller sub-problems. Future studies should consider mechanisms for more equitably distributing delays amongst all flights being scheduled.

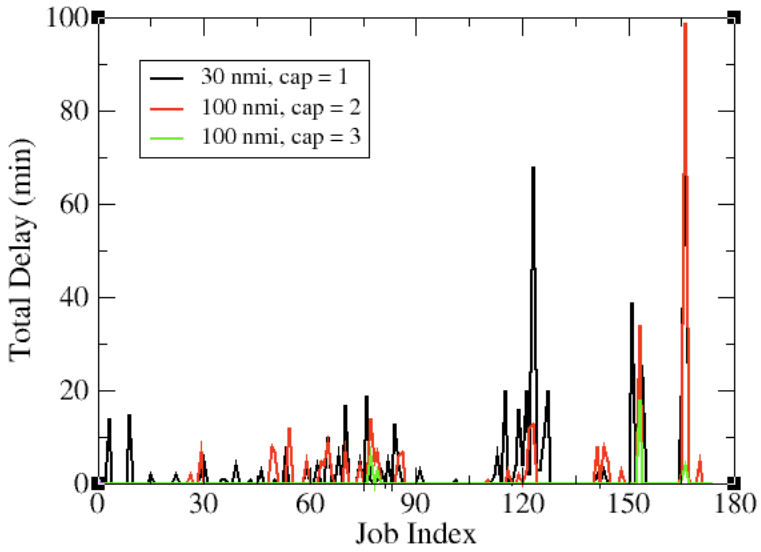

Figure 6. Total delays per job for (1) 30 nmi grid, six sub-problem, capacity=1; (2) 100 nmi, six sub-problems, capacity =2; and (3) 100 nmi grid, six sub-problems, capacity=3.

IV. Conclusions

This paper contains the results of the first extensive study designed to assess the impact of strategically scheduling flights on user-preferred routes in the Central East Pacific in order to reduce or eliminate the number of trajectory crossing points. These crossing points were identified in a previous study as a source of concern due to

the controller workload associated with ensuring the safe separation of these flights in the oceanic environment. Minimum-time, wind-optimal routes were used as a surrogate for the actual user-preferred routes.

To accomplish the flight scheduling, an innovative technique was used to cast the original air traffic flow problem in terms of a job shop scheduling problem. A 0-1 integer programming model was then used to calculate the optimal departure and en route delays necessary to generate feasible flight schedules. The computational tractability of the flight scheduling model was enhanced by utilizing a ration-by-schedule based heuristic to partition the original scheduling problem into *N* sub-problems.

By varying attributes of the machines in the job shop scheduling formation, two distinct types of feasible schedules are obtained. The first type of schedules, which rely on the 30 nmi x 30 nmi machines, are highly restrictive but free of all trajectory crossing points, while the second type, which rely on the 100 nmi x 100 nmi machines, are less restrictive but may require limited tactical flight separation maneuvers to alleviate residual crossing points. After allowing user-preferred routes and strategically reducing the number of 4-D trajectory crossing points, the adjusted per flight time savings varied between 1.8 minutes and 4.6 minutes, respectively, depending on the size of the airspace (i.e., either 30 nmi x 30 nmi or 100 nmi x 100 nmi) associated with the machines in the job shop scheduling problem. The estimated annual economic benefit to the airlines was found to vary between $3.4 million and $8.5 million when wind-optimal routing and strategic flight scheduling was introduced into the CEP.

Finally, future extensions to this study will examine the development of sparse grids that take advantage of the prevailing traffic patterns in the CEP in order to reduce computational complexity. In addition, more sophisticated multi-objective cost functions that equitably distribute delays will be examined, as will simpler heuristic based scheduling methodologies.

References

[1]Joint Planning and Development Office, "Concept of Operations for the Next Generation Air Transportation System, Version 0.2," URL: http://techhangar.jpdo.aero/ [Cited Jan. 25, 2007].

[2]Brewer-Dougherty, T., Colamosca, B., Elsayed, E.A., Gerhardt-Falk, C., Livingston, D., Martin, L., and Schroepfer, C., "Modeling and Simulation of Air Traffic Changes in the Northern Pacific Airspace: Investigation of the Effects on System Performance," *Air Traffic Control Quarterly*, Vol, 14, No. 2, 2006, pp. 139-157.

[3]Williams, A., Mondoloni, S., Western, R., Karakis, and Karakis, T., "Application of Airborne Systems for Improving North Atlantic Organized Track System Operations," *AIAA 5th Aviation, Technology, Integration, and Operations Conference*, Arlington, VA, Sept. 26-28, 2005.

[4]Grabbe, S., Sridhar, B., and Cheng, N., "Central East Pacific Flight Routing," *AIAA Guidance, Navigation, and Control Conference*, Keystone, CO, Aug. 21-14, 2006.

[5]Brucker, P., *Scheduling Algorithms,* 2nd ed., Springer-Verlag, Heidelberg, Germany, 1998.

[6]Bertsimas, D. and Patterson, S.S., "The Air Traffic Flow Management Problem with Enroute Capacities," *Operations Research*, Vol. 46, No. 3, May-June 1998.

[7]Manne, A.S., "On the Job-Shop Scheduling Problem," *Operations Research*, Vol. 8, No. 2, Mar.-Apr. 1960.

[8]Pinedo, M.L., *Planning and Scheduling in Manufacturing and Services*, Springer Science+Business Media, Inc., New York, NY, 2005.

[9]Gupta, A.K. and Sivakumar, A.I., "Job shop scheduling techniques in semiconductor manufactoring," *International Journal of Advanced Manufacturing Technology*, Vol. 27, pp. 1163-1169, 2006.

[10]Green, S.M., Bilimoria, K.D., and Ballin, M.G., "Distributed Air-Ground Traffic Management for En Route Flight Operations," *AIAA Guidance, Navigation, and Control Conference*, Denver, CO, Aug. 14-17, 2000.

[11]Sridhar, B. and Chatterji, G.B., "Computationally Efficient Conflict Detection Methods for Air Traffic Management," Proceedings of the American Control Conference, Albuquerque, NM, June, 1997.

[12]Jardin, M.R., "Grid-Based Strategic Air Traffic Conflict Detection," *AIAA Guidance, Navigation, and Control Conference*, San Francisco, CA, Aug. 15-18, 2005.

[13]"Enhanced Traffic Management System (ETMS)," Report No. VNTSC-DTS56-TMS-002, Volpe National Transportation Center, U.S. Dept. of Transportation, Cambridge, MA, Oct. 2005.

[14]"Aircraft Situation Display To Industry: Functional Description and Interface Control Document," Report No. ASDI-FD-001, Volpe National Transportation Center, U.S. Dept. of Transportation, Cambridge, MA, June 29, 2005.

[15]"EMC Model Documentation," National Centers for Environmental Predictions, National Oceanic and Atmospheric Administration, URL: http://www.emc.ncep.noaa.gov/modelinfo/ [Cited Jan. 25, 2007].

[16]"Economic Values for FAA Investment and Regulatory Decisions, A Guide," Contract No. DTFA 01-02-C00200, GRA, Inc., Prepared for FAA Office of Aviation Policy and Plans, U.S. Federal Aviation Administration, Washington, DC, Dec. 2004.